Neurocomputing ∎ (∎∎∎∎) ∎∎∎–∎∎∎

Contents lists available at ScienceDirect

Neurocomputing

journal homepage: www.elsevier.com/locate/neucom

Local quality assessment of point clouds for indoor mobile mapping

Fangfang Huang [a], Chenglu Wen [a,*], Huan Luo [a], Ming Cheng [a], Cheng Wang [a], Jonathan Li [a,b]

[a] Fujian Key Laboratory of Sensing and Computing for Smart Cities, Xiamen University, Xiamen 361005, China
[b] Department of Geography and Environmental Management, University of Waterloo, Waterloo, ON N2L 3G1, Canada

ARTICLE INFO

Article history:
Received 2 November 2015
Received in revised form
17 January 2016
Accepted 21 February 2016

Keywords:
Local quality assessment
Indoor mobile mapping
Point clouds
Degradation
Machine learning

ABSTRACT

The quality of point clouds obtained by RGB-D camera-based indoor mobile mapping can be limited by local degradation because of complex scenarios such as sensor characteristics, partial occlusions, cluttered backgrounds, and complex illumination conditions. This paper presents a machine learning framework to assess the local quality of indoor mobile mapping point cloud data. In our proposed framework, a point cloud dataset with multiple kinds of quality problems is first created by manual annotation and degradation simulation. Then, feature extraction methods based on 3D patches are treated as operating units to conduct quality assessment in local regions. Also, a feature selection algorithm is deployed to obtain the essential components of feature sets that are used to effectively represent local degradation. Finally, a semi-supervised method is introduced to classify quality types of point clouds. Comparative experiments demonstrate that the proposed framework obtained promising quality assessment results with limited labeled data and a large amount of unlabeled data.

1. Introduction

Indoor 3D models are essential sources in acquiring information for many applications such as earthquake rescue tasks, cultural heritage protection, and intelligent building design. The quality and accuracy of creating an indoor 3D model are influenced by the quality of data collected from the real world. Point cloud data, a way to describe the 3D indoor environment, are widely exploited in building indoor 3D models [1–5]. With the rapid development of indoor mobile mapping systems (IMMSs), many IMMSs have been used to collect indoor point cloud data [6–10]. Typical IMMSs include wheeled mobile systems, backpacked mobile systems, and hand-held devices, etc. The wheeled mobile system smoothly integrates multi-sensors, including cameras, laser scanners, and inertial measurement units on a mobile platform, e.g., pushcart or robot. In the backpacked mobile system, the user backpacks a multi-sensor integrated system to collect data in motion. In the hand-held system, a data acquiring device, e.g., Kinect, is held by users when acquiring data. This way, it is convenient for these hand-held devices to collect data under certain conditions, especially in areas that are difficult for other IMMSs to access. In our proposed framework, the dataset is collected by a Kinect camera mounted on a mobile robot [7].

Some quality problems, or data degradation, such as missing data, occluded data, sparse data, blurred data, and very dark or very bright data, are inevitable for IMMS point clouds. Causes of data degradation include the characteristics of the sensing device, large rotation angle of the mobile platform in motion, and uneven illumination distribution in an indoor environment. Compared with image degradation, the reasons for the degradation of point clouds differ in different local areas, leading to an uneven distribution of point cloud quality. Moreover, different reasons of degradation lead to a diverse degradation of point clouds. Therefore, the qualities of point clouds have the characteristics of diversity and locality for indoor mobile mapping.

The local quality assessment of point clouds are to handle the data quality assessment by considering the diverse and local degradation of the IMMS point clouds. In general, good indoor point cloud data should not only have complete structure information but also maintain consistency between the appearance and structural information. Poor quality data need to be discriminated because they will not provide effective and sufficient information. However, in our dataset, there is an imbalanced problem, i.e., the amount of low-quality data is much greater than high-quality data. The local quality assessment of point clouds can classify these data into different degradation types and prepare for the further repair of these data based on different strategies. One main challenge for automated quality assessment of IMMS point clouds is the

* Corresponding author.
E-mail addresses: huangfangfang2013@foxmail.com (F. Huang), clwen@xmu.edu.cn (C. Wen), scholar_luo@163.com (H. Luo), chm99@xmu.edu.cn (M. Cheng), cwang@xmu.edu.cn (C. Wang), junli@uwaterloo.ca (J. Li).

http://dx.doi.org/10.1016/j.neucom.2016.02.033
0925-2312/

establishment of a training dataset in terms of time and cost. On one hand, it is difficult to classify different quality types in one point cloud by manually labeling because of the diverse and local degradation of point clouds. On the other hand, it is difficult, or impossible, to obtain the ground-truth (or reference data) without degradation, which indicates that our quality assessment problem needs to be considered in the absence of reference situations. Thus, it is essential to know how to use limited labeled data to predict the labels of a large number of unlabeled data. A semi-supervised learning method, i.e., a method requiring only a small amount of labeled training data, provides an efficient way to address this challenge.

In this paper, we propose a new framework to assess the local quality of indoor mobile mapping point clouds. First, we describe the IMMS point cloud degradation by geometric feature descriptors. To effectively analyze the essential components of these geometric feature descriptors, a feature selection method is integrated into the proposed framework to reduce the redundancy of these used features. To avoid the intensive labor costs of manual labels, a semi-supervised method, named Safe Semi-supervised Support Vector Machines (S4VMs) [11], is integrated into our proposed framework to conduct quality assessment tasks by manually labeling a small portion of the training dataset. Additionally, we establish a point cloud dataset (benchmark) with multiple kinds of quality problems to evaluate the proposed framework.

The rest of this paper is organized as follows: first, Section 2 reviews the related work; next, Section 3 details our proposed framework in three parts, including the establishment of a dataset with multiple kinds of quality problems, the feature description of the degraded data, and the local quality assessment of indoor point clouds; then, Section 4 reports the experimental results and presents the comparative experiments; finally, Section 5 concludes the entire paper.

2. Related works

Most recent works on data quality assessment focused on 2D images [12–16]. Xue et al. [12] established a codebook to assess the quality of images by computing quality-aware centroids of each patch in the training images. Ref. [13] presented a sparse feature representation method to learn a dictionary on the spatial correlations between training images. Two deep neural network methods in Refs. [15] and [16] were introduced to address non-referenced image quality assessment by incorporating a semi-supervised method and multi-scale directional transform, respectively. Compared with the great achievements of image quality assessment, the quality assessments of point clouds have been mainly focused on positioning accuracy [17–20]. Sander et al. [17] analyzed the relationships between the geometric quality of input point cloud data and the corresponding generated 3D models. In [18], a deviation analysis between the building information models and point cloud data was proposed to assess the quality of the models. In [19], the quality assessment of point clouds was considered as a spatial structure projection in coordinate planes and positioning accuracy, which represented the deviation between sign coordinates collected by a laser scanner and precise coordinates collected by the total station. Many researchers have conducted investigations on the quality assessment of Kinect depth data in recent years [21–22]. However, few research results have presented a systematic quality assessment of IMMS point clouds, thus raising the demand to establish a suitable benchmark for IMMS point cloud quality assessment metrics.

In the past decades, semi-supervised learning has attracted increasing attention [23–31] because only a part of the sample is required to be manually labeled for learning a statistical model. In [23], semi-supervised discriminant analysis (SDA) was exploited for both labeled and unlabeled data to reduce the dimensionality. Yu et al. [24] presented an adaptive hypergraph method for image classification by simultaneously learning the labels of unlabeled data and optimizing the weights of hyperedges. In [25], a stochastic learning method was proposed to address the image classification problem by acquiring a high-order distance from hypergraph and integrating labeling information from different views. Liu et al. [28] proposed a hypergraph model with adaptive probability to find related media content for media event enrichment task. In [27,30], and [31], hypergraph combined with sparse representation was introduced to address prediction or classification problems. In [11], S4VMs were presented to generate a multiple low-density separator pool and to maximize the performance of each candidate separator. S4VMs mainly focused on producing a safe model by a training dataset containing both labeled and unlabeled data. Compared with other methods, S4VMs have the advantage of a safe generalization performance. The safe of S4VMs is that its generalization performance is never statistically significantly worse than these fully supervised methods. In our proposed framework, we only use a small portion of labeled data to reduce labor costs and exploit S4VMs for considering both labeled and unlabeled data to learn a statistical classifier for quality assessment tasks.

3. Proposed method

3.1. Point clouds acquisition

An IMMS integrating a 2D laser scanner and a RGB-D camera is adopted for collecting 3D indoor point clouds in this paper [7]. The 2D laser scanner and RGB-D camera are used to build 2D map and to obtain point clouds, respectively. Moreover, this IMMS can achieve a 2D trajectory of the mobile platform while building the maps. However, the acquired data have some quality problems, such as missing data, occluded data, too sparse data, blurriness, and too much darkness or brightness. To deeply delve into these problems, the main reasons that lead to data degradation are detailed as follows.

The characteristics of the Kinect sensor include the limited measurement range of the sensor and the low image resolution of the camera (Fig. 1(a)). Unlike a hand-held camera system, our mobile robot-based IMMS acquires data while exploring the environment. In this case, when the moving speed of the mobile robot is too fast, data quality may be decreased because it is difficult to ensure that the RGB and depth images are synchronous. This RGB information drift may result in blurred data (Fig. 1(b)). Moreover, when the mobile robot is too close to (or too far away from) perceived objects in the measuring range, the acquired data density will be too dense (or too sparse) (Fig. 1(c)). Uneven illumination in an indoor environment is shown in Fig. 1(d). For example, some place may separate into different areas with different illumination conditions by object occlusions or by being close to (or far away form) the light source when acquiring data in motion. Certain perceived objects, such as transparent and refractive objects (e.g., glass, monitors, etc.), possess obvious degraded quality problems, while the smooth surfaces and non-refractive objects are almost invisible (Fig. 1(e)). The structure and feature details of the perceived objects are incomplete (Fig. 1(f)). For example, the bent arm of a chair will not be detected because of its irregular structure. Furthermore, detailed structural information of a small table pot will be missing because of the complicated structure of the pot.

Please cite this article as: F. Huang, et al., Local quality assessment of point clouds for indoor mobile mapping, Neurocomputing (2016), http://dx.doi.org/10.1016/j.neucom.2016.02.033

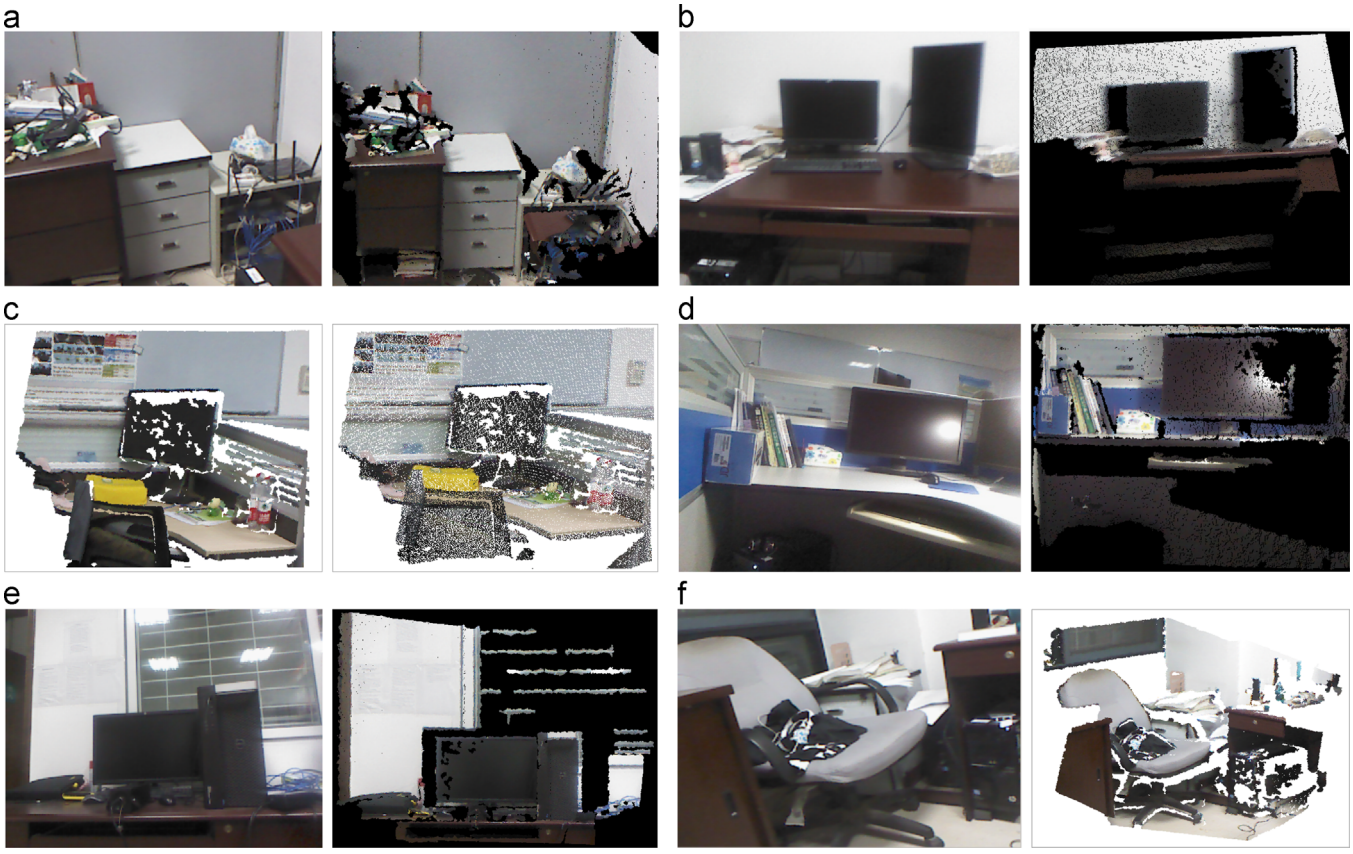

Fig. 1. Examples of degradation in IMMS point cloud data. (a) Data missing due to the low image resolution of the camera. (b) Data blurred due to the fast moving speed of the mobile platform. (c) Sparse data due to the far distance from the mobile platform to the perceived objects. (d) Data missing due to the uneven illumination. (e) Data missing due to the surface characteristics of the perceived objects. (f) Data missing due to the complicated structure and feature details of the perceived objects.

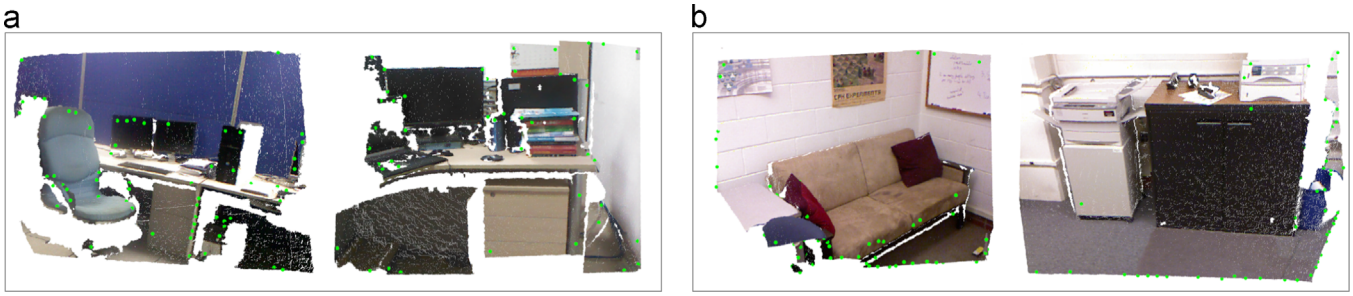

Fig. 2. Green points represent the NARF key points extracted. (a) 61 and 45 NARF key points extracted from two our data. (b) 63 and 54 NARF key points extracted from two Cornell data [37–39]. (For interpretation of the references to color in this figure legend, the reader is referred to the web version of this article.)

3.2. Feature description

In the proposed framework, geometric feature descriptors are used to describe the IMMS point cloud data. To effectively analyze the essential components of these geometric feature descriptors, a feature selection method is integrated into the proposed framework to reduce the redundancy of these used features. In the remainder of this section, both feature extraction and selection are detailed.

In the feature extraction stage, it is observed that the point clouds from corner and edge regions are vulnerable for degradation during acquisition. In practice, 3D patches are treated as operating units to conduct quality assessment in local regions. Therefore, we first extract key points using the normal aligned radial feature (NARF) [32] method (see Fig. 2). Then, each key point based on a 3D patch is described by a geometric feature set, including fast point feature histograms (FPFH) [33], spin image [34], spectral features [35], orientation of spectral feature, and bounding box. Specifically, the FPFH and spin image use a statistical way to output all results to histograms. Spectral features [35] capture the scatter-ness, linear-ness and flat-ness of the local geometry of the point distribution. Orientations, i.e., directions against the vertical and horizontal planes, are used as the directional features. The bounding box descriptor calculates the eigenvalues of the principle, middle, and smallest eigenvectors in the principal component space [36].

In the feature selection stage, the importance of feature components in these extracted geometric features is measured and analyzed [40–42]. Because the redundancy of features in the feature set may influence the performance of these classifiers such as SVM and random forest. Here, the importance $\overline{D}_j$ of the jth bin in feature set (variable importance) is used as an indicator to measure the importance of the corresponding feature component. It is

Please cite this article as: F. Huang, et al., Local quality assessment of point clouds for indoor mobile mapping, Neurocomputing (2016), http://dx.doi.org/10.1016/j.neucom.2016.02.033

computed as follow:

$$\overline{D}_j = \frac{1}{B}\sum_{b=1}^{B}(R_b - R_{b_j}) \quad (1)$$

where R_b is the number of correct classifications while R_{b_j} is the number of correct classifications without considering the jth feature. B is the number of instances. Eq. (1) determines the score of variable importance. Therefore, the rank of variable importance is obtained by these scores. Besides, an optimized feature subset can be built by reducing the features with low importance scores from this rank. Finally, these selected features are adopted as a new feature set to train a learning model.

3.3. Quality assessment by a semi-supervised framework

The quality assessment of IMMS point clouds is a challenging task because it is time consuming to obtain a large amount of labeled data. Also, the reference data are difficult to obtain without degradation. To recognize the quality types, our local quality assessment is considered as quality type classification. Here, we choose a S4VM method [11] to solve classification problem because of its safe generalization performance. S4VM trains the model with limited labeled data and a large amount of unlabeled data. Compared to SVM, S4VM has following two advantages. First, S4VM is rarely inferiors to SVM on classification accuracy because it fully exploits the unlabeled data based on SVM in the training process; second, S4VM has the advantage of higher robustness because of its multiple representative separators. The representative separators of S4VM is that these separators not only have large-margin decision boundary but also pass through the low-density regions of data distribution. In our experiments, these representative separators are extracted by adopting K-means algorithm [43]. We briefly introduce the principal of S4VM here, and give the details for integrating S4VM into our quality assessment framework.

Formally, a binary classification is defined here. Given a training dataset $D_n = \left\{\{x_i, y_i\}_{i=1}^{l} \cup \{x_j\}_{j=l+1}^{l+u}\right\}$, where l represents labeled quality instances and u represents unlabeled quality instances. Denote $Y = \{y_n \in \pm 1\}_{n=1}^{l+u}$ as the label space of quality instances, whereas $\{+1\}$ represents the positive quality type and $\{-1\}$ represents the other negative quality types. And, let $y = \left\{y_{l+1}, \ldots, y_{l+u}\right\} \in \mathcal{B}$ be the label assignment of unlabeled quality instances. Here $\mathcal{B}$ is a set of label assignments in Eq. (2):

$$\mathcal{B} = \left\{ y \in \{\pm 1\}^u \left| -\beta \le \frac{\sum_{j=l+1}^{l+u} y_j}{u} - \frac{\sum_{i=1}^{l} y_i}{l} \le \beta \right.\right\} \quad (2)$$

where β is a constant to control the proportion of positive and negative samples. Thus, the quality assessment aims to find the optimal label assignment $\bar{y}$ with the least cost of objective function. The objective function of a representative separator is described in Eq. (3):

$$h(f,\hat{y}) = \frac{1}{2}\|f\|^2 + C_1\sum_{i=1}^{l} L(y_i, f(x_i)) + C_2\sum_{j=l+1}^{l+u} L(\hat{y}_j, f(x_j)) \quad (3)$$

where the function $f: X \to Y$ and function $L(Y, f(X))$ compute the hinge loss on SVM. C_1 and C_2 are two constants denoting impact factors. If C_2 is equal to 0, the model will degenerate to inductive SVM.

To search for a pool of diverse representative separators $\{f_t\}_{t=1}^{T}$ and their corresponding label assignments $\{\hat{y}_t\}_{t=1}^{T}$, the optimal objective function of S4VM model is given in Eq. (4):

$$min_{\{f_t, \hat{y}_t \in \mathcal{B}\}_{t=1}^{T}} \sum_{t=1}^{T} h(f,\hat{y}_t) + M\Omega(\{\hat{y}_t\}_{t=1}^{T}) \quad (4)$$

where Ω is a penalty function used to measure the diversities of the separators. T is the number of separators while M is a large constant to guarantee large diversities. In our experiments, T and M are set at 10 and 10^5. In this process, K-means algorithm is exploited to extract T representative separators. Meanwhile, the value of K is equal to T. Thus, each cluster outputs a representative separator with a minimum objective value. To determine the optimal separator, Eqs. (5–7) are applied to evaluate these representative separators.

$y, \hat{y}$ *and* y^{SVM} are denoted as the goal of label assignment, the label assignment of S4VM model, and the label assignment of inductive SVM, respectively. Set $gain(y,\hat{y},y^{SVM})$ and $loss(y,\hat{y},y^{SVM})$ as the gained and loss functions:

$$\begin{aligned} gain(y,\hat{y},y^{SVM}) &= \sum_{j=l+1}^{l+u} I\left(y_j = \hat{y}_j\right) I\left(\hat{y}_j \neq y_j^{SVM}\right) \\ &= \sum_{j=l+1}^{l+u} \frac{1+y_j\hat{y}_j}{2}\frac{1-y_j^{SVM}\hat{y}_j}{2}. \end{aligned} \quad (5)$$

$$\begin{aligned} loss(y,\hat{y},y^{SVM}) &= \sum_{j=l+1}^{l+u} I\left(y_j \neq \hat{y}_j\right) I\left(\hat{y}_j = y_j^{SVM}\right) \\ &= \sum_{j=l+1}^{l+u} \frac{1-y_j\hat{y}_j}{2}\frac{1+y_j^{SVM}\hat{y}_j}{2}. \end{aligned} \quad (6)$$

To obtain the maximized gained function value and the minimized loss function value under identical situations, Eq. (7) is proposed as follows:

$$max_{y \in \mathcal{B}}\, gain(y,\hat{y},y^{SVM}) - \lambda\, loss(y,\hat{y},y^{SVM}) \quad (7)$$

where λ is a constant (e.g., 3 in our experiment) to control the degree of risk. As there are multiple representative separators, the optimal separator is the one that can achieve the optimal solution. The final prediction, denoted as $\bar{y}$, is given by:

$$\bar{y} = \arg max_{y \in \mathcal{B}} min_{\hat{y} \in \{\hat{y}_t\}_{t=1}^{T}}\, gain(y,\hat{y},y^{SVM}) - \lambda\, loss(y,\hat{y},y^{SVM}) \quad (8)$$

To generate the label assignment $\bar{y}$, the label assignment of unlabeled quality instances y is first generated randomly. Then, the predicted labels y are continuously updating under iterations. Meanwhile, K-means algorithm is used to search for multiple representative separators. On a iteration, a new S4VM model should be updated based on $y, \hat{y}$ *and* y^{SVM}. Thus, the performance of S4VM is improved and is rarely inferior to that of inductive SVM. Finally, the optimal representative separator with the smaller value of objective function is determined using Eq. (8). Furthermore, the labels with unlabeled quality instances can be obtained in $\bar{y}$ for quality assessment.

4. Experiments and results

The proposed framework was coded with C++, and implemented on a personal computer with a single core 3.2 GHz and a RAM of 16 GB. To assess the data quality of local regions of a point cloud, the local search radius of 3D patch is set to 6 cm. According to [11], the regularization parameters C_1, C_2, and β, are set to 100, 0.1 and 0.1, respectively. Besides, the sampling size N, cluster number T, and risk parameter λ, are set to 100, 10, 3, respectively. The kernel type of S4VM is KBF.

4.1. Experimental data

Our experiments are performed on two datasets: Cornell RGB-D dataset [37–39] and our dataset collected by the system [7] (dataset available on: http://rssi.xmu.edu.cn/contents/download_en.html). In this paper, we focus on the good type and two degraded types. Each dataset contains three quality types of point clouds, namely good, missing, and sparse types (see Fig. 3). The good type not only have complete structure information but also maintain consistency between the appearance and structural information. The missing type miss structure information. The

Please cite this article as: F. Huang, et al., Local quality assessment of point clouds for indoor mobile mapping, Neurocomputing (2016), http://dx.doi.org/10.1016/j.neucom.2016.02.033

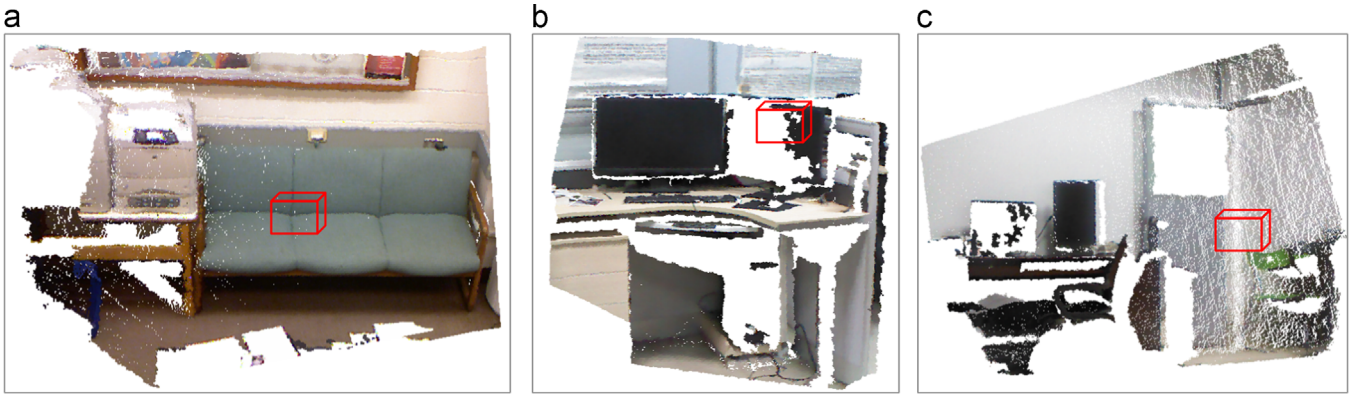

Fig. 3. Three quality types in our dataset and the Cornell dataset. (a) Good type. (b) Missing type. (c) Sparse type.

Table 1
Instances of our dataset and the Cornell RGB-D dataset.

Samples	Our dataset			Cornell RGB-D dataset		
	Good	Missing	Sparse	Good	Missing	Sparse
Positive	804	1140	1140	1000	900	1200
Negative	804	1140	1140	1000	900	1200
Total	1608	2280	2280	2000	1800	2400

sparse type have an uneven density of points in a local region. In particular, the sparse type can also be obtained from the good type point clouds by a simulation method, i.e., we use a uniform sampling filter to reduce the number of points and maintain the geometric shape of the point cloud in the PCL1.7.2 library [44].

The instances from the two datasets are shown in Table 1. The negative instances of one quality type point cloud consist of the other two quality types' point cloud instances with an equal number. For example, the number of the good type's positive instances is 804 in our dataset; thus, its negative instances consist of 402 missing instances and 402 sparse instances. In the Cornell dataset, the total instances of good, missing, and sparse types are 2000, 1800, and 2400, respectively. In our dataset, the total instances of good, missing, and sparse types are 1608, 2280, and 2280, respectively.

4.2. Variable importance analysis

In our experiments, FPFH (16 dimensions), spin image (208 dimensions), spectral feature (three dimensions), orientation (two dimensions), and bounding box (three dimensions) descriptors are extracted as a feature set (in that order). Thus, a 232 dimensional feature set was extracted at the NARF key points in a local region of each point cloud based on 3D patches. Afterwards, to reduce some unimportant or noisy components of the features, we use random forest algorithm to analyze variable importance of bins in feature set. Based on the variable importance estimation, we select the significant bins in feature set with high scores of variable importance.

To select the essential components of the features, we first apply Eq. (1) to compute the importance score of bins in feature set (variable importance). Fig. 4(a) and (b) shows the variable importance scores of the good, missing, and sparse quality types on our dataset and the Cornell dataset, respectively. In Fig. 4, the higher the variable importance is, the more important the corresponding bin is to classify the defined three quality types from each other. We observe that the variable importance scores have obviously difference among three quality types at the same bin in the feature set. Except for the sparse type in the Cornell dataset, a commonality exists in the other quality types is that the first sixteen bins in the feature set (which represents FPFH descriptors) have lower variable importance, which causes the corresponding features will be reduced in the next feature selection process. The main reason is that FPFH descriptors are computed rapidly using global and local information, and global information will lead to some similar feature variables in most key points. Additionally, the spectral shape, orientation, and bounding box descriptors, namely the last eight bins, have relatively high variable importance and are regarded as very important features in the feature selection process. In Fig. 4(a) and (b), the variable importance of FPFH in the Cornell dataset's sparse type obtains a higher score than the variable importance of FPFH obtained in other quality types among the two datasets. Because the objects' structure is damaged after degradation simulation. In the spin image descriptors (bins from 17 to 225), the variable importance of bins in our dataset and the Cornell dataset obtains rather different scores. Hence, we conclude that different datasets and quality types lead to different variable importance at a same bin in feature set. Thus, feature selection is a significant process to select discriminated features for the quality assessment task.

To verify the effectiveness of selected features with high variable importance scores, we construct an optimal feature subset for the quality assessment task by computing the accumulated variable importance. Here, the accumulated variable importance adds up the variable importance scores of selected bins which have top ranking in all bins. Fig. 5 shows the relationship between the feature number selected and the corresponding accumulated variable importance for the defined three quality types. In the four figures, the blue, red and green lines represent good, missing and sparse quality types, respectively. As shown in Fig. 5(a), the good type has a higher accumulated variable importance than other two quality types using selected features with numbers ranging from 20 to 75. On the contrary, the sparse type has the lowest accumulated variable importance among three types. From this result, we deduce that the good type is easier to be identified than the others, and the sparse type is the most difficult to be identified. Compared to the curve which feature number selected is smaller than 60, when the feature number selected is larger than 60, all the three curves present relatively smaller increase. Besides, the accumulated variable importance scores of 60 feature number selected are larger than 0.5 in all the three curves. For the selected features with numbers of 30, 45, and 60, the corresponding accumulated variable importances of good type are 0.52, 0.64, and 0.72, respectively; on the other hand, the sparse types obtains 0.44, 0.54, and 0.62, respectively. The above results illustrate that 60 numbers of the selected feature are sufficient for the identification tasks in our dataset. In Fig. 5(b), the accumulated variable importances of the sparse type are the highest while the

Please cite this article as: F. Huang, et al., Local quality assessment of point clouds for indoor mobile mapping, Neurocomputing (2016), http://dx.doi.org/10.1016/j.neucom.2016.02.033

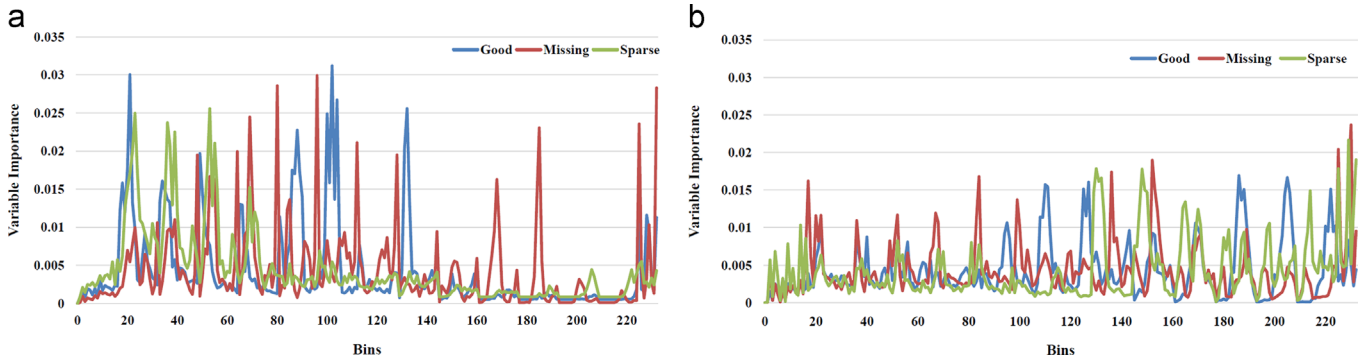

Fig. 4. The variable importance of each bin on good, missing, and sparse quality types. (a) Our dataset. (b) Cornell dataset.

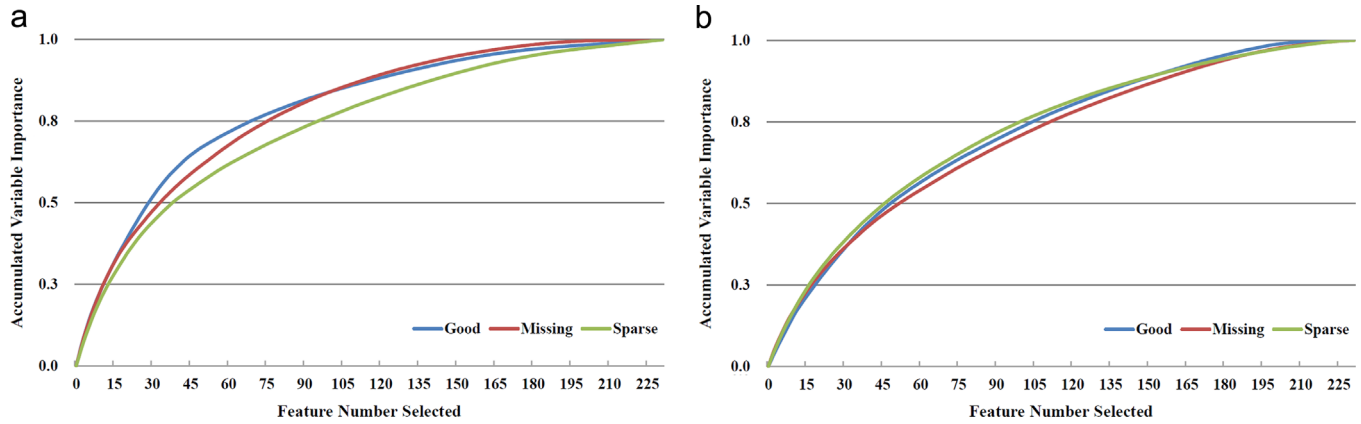

Fig. 5. The relationship between the feature number selected and the corresponding accumulative variable importance on good, missing, and sparse quality types. (For interpretation of the references to color in this figure, the reader is referred to the web version of this article.)

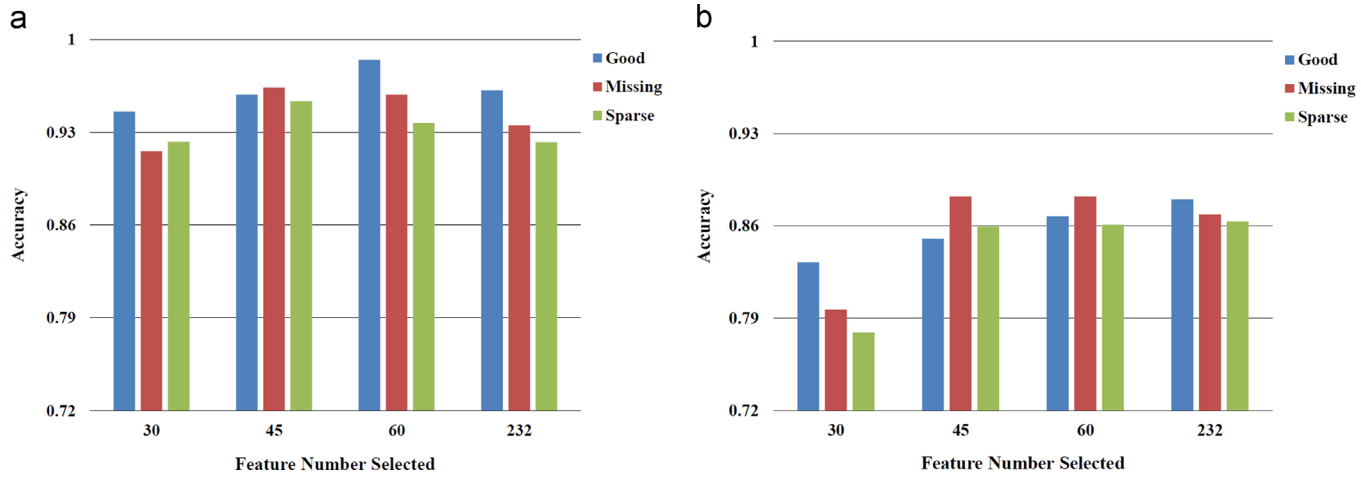

Fig. 6. The accuracies of feature number selected on good, missing, and sparse quality types with 50 labeled data. (a) Our dataset. (b) Cornell dataset.

accumulated variable importances of the missing type are the lowest. For feature numbers of 30, 45, and 60, the corresponding accumulated variable importances of the sparse type are 0.38, 0.49, and 0.58, respectively; on the other hand, the corresponding accumulated variable importances of the missing type are 0.36, 0.46, and 0.54, respectively. The accumulated variable importances of 60 feature number selected are larger than 0.5 in all the three curves. The above results in Fig. 5(b) also illustrate that 60 feature number selected are sufficient for the identification tasks in the Cornell dataset. To obtain the best performance, we finally test the best feature subsets with 30, 45, and 60 dimensions as the training data for the quality assessment task.

4.3. Model parameter effect on assessment

To evaluate our proposed framework, we introduced four evaluation measurements, including accuracy, precision, recall, and F_1-measure. In our experiments, we focused on testing the influence of feature number selected and the number of labeled training data on our quality assessment results. Fig. 6 shows the influence of different feature number selected on accuracy measurement when 50 labeled training data are used. In our dataset, for the missing and sparse types, the highest score is achieved when 45 dimensions of feature subset is selected, while the similar results are obtained in the Cornell dataset. For the good

Please cite this article as: F. Huang, et al., Local quality assessment of point clouds for indoor mobile mapping, Neurocomputing (2016), http://dx.doi.org/10.1016/j.neucom.2016.02.033

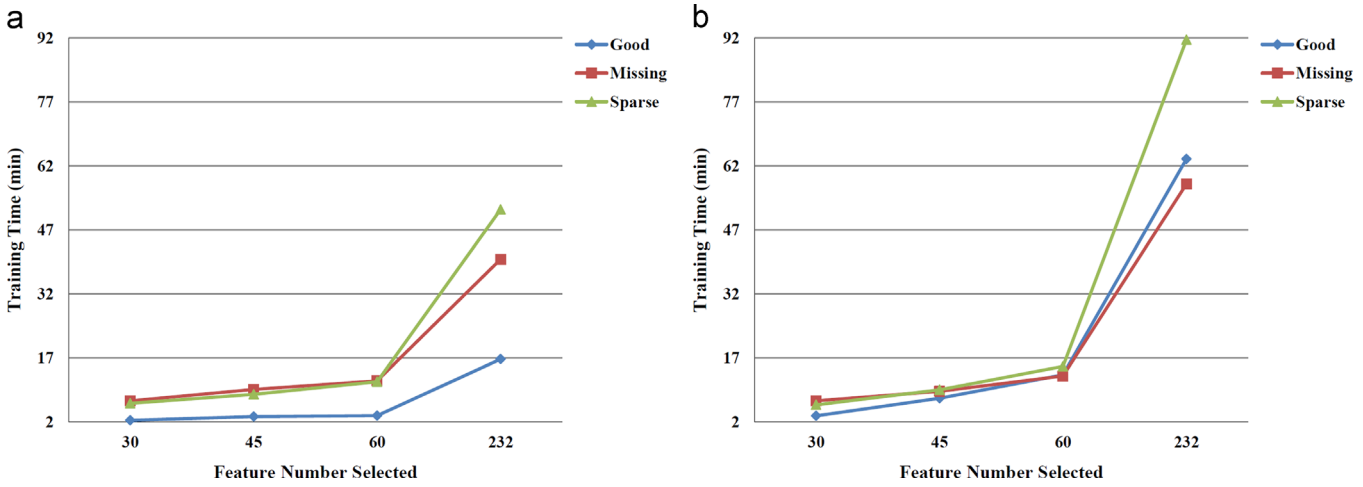

Fig. 7. The training time *vs.* feature number selected on good, missing, and sparse quality types with 50 labeled data. (a) Our dataset. (b) Cornell dataset.

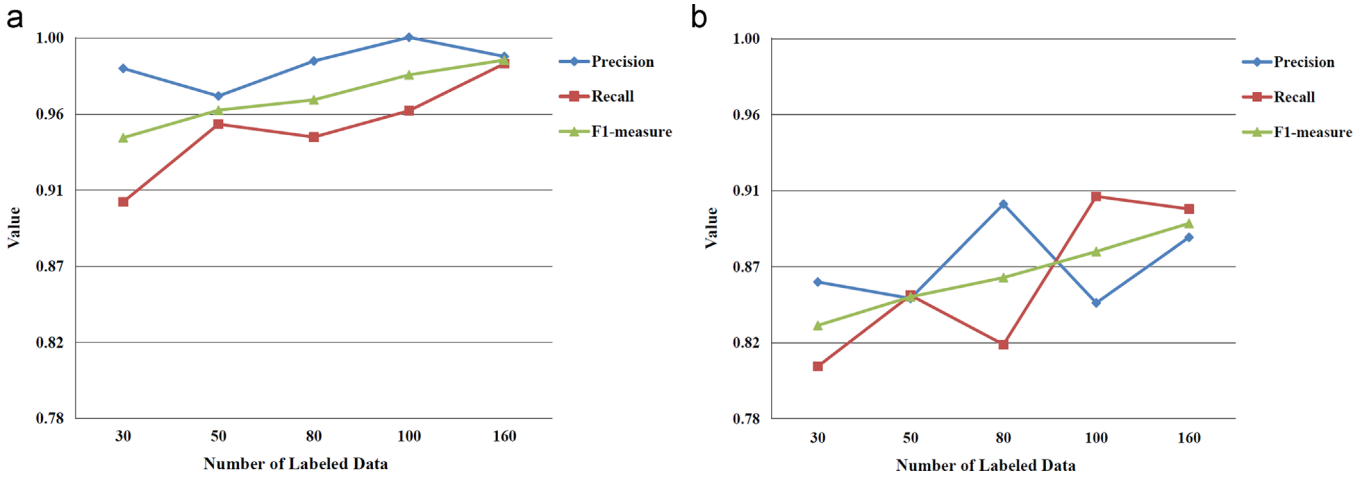

Fig. 8. The precision, recall, and F_1-measure using different numbers of labeled data on the good type. (a) Our dataset. (b) Cornell dataset.

type, the optimal feature subset with 60 dimensions achieves the highest score in our dataset compared to the optimal feature subset with 232 dimensions in the Cornell dataset. As a conclusion, when the optimal feature subset with 60 dimensions is used, the test results on our dataset and the Cornell dataset have achieved accuracies higher than 93% and 86%, respectively. The achieved accuracies prove that the optimal feature sets with dimensions of 45 and 60 are enough to achieve satisfactory assessment results after our feature selection process. The above analyses show that the feature selection method is effective for the proposed quality assessment framework.

Fig. 7 represents the training time for the good, missing and sparse types with different feature number selected when 50 labeled training data are used. As illustrated in Fig. 7, as the feature number selected decreases, the training time declines. Thus, to improve the time efficiency of proposed framework, it is very important to select a significant feature subset to reduce the feature dimensions. Comprehensively considering time efficiency and classification accuracy, we finally chose an optimal feature subset with 45 dimensions as the input of training data for our assessment task.

To analyze the influence of the number of labeled data on assessment results, we used the optimal feature subsets of the quality types with fixed 45 dimensions. Figs. 8–10 shows precision, recall, and F1-measure of our method with different number of labeled training data. In Figs. 8–10, five settings of labeled training data are used to present the experimental results of all the three quality types with 45 feature number selected. In all these figures, the horizontal axis represents the number of labeled training data, i.e. 30, 50, 80, 100, and 160 labeled data. Meanwhile, the remainder of the unlabeled data are also used for the training model. As illustrated in Figs. 8–10, three measurements: precision, recall, and F_1-measure, vary with the number of labeled data used in training our S4VM model on classifying the good, missing and sparse types. The value of F_1-measure ascends with the increase of labeled data when classifying the good types (see Fig. 8). Moreover, the values of F_1-measure staying above 0.93 on our dataset and 0.83 on the Cornell dataset show the stable performance of S4VM in our proposed framework. As seen in Fig. 9, the F_1-measure of the missing type changes slightly as the number of labeled data increases on our dataset. On the Cornell dataset, the F_1-measure of the missing type increases obviously from 0.79 to 0.89 when the number of labeled data ranges from 30 to 50. In Fig. 10, the F_1-measure illustrates that S4VM model has a stable performance with the value staying above 0.86 for the sparse types on our and the Cornell dataset. Thus, we can conclude that the number of labeled data is a significant factor to classify the quality types in the proposed framework.

To assess the performance of proposed framework, we analyzed the impact of the number of labeled data on the corresponding training time when classifying the quality types in Fig. 11. As illustrated in Fig. 11(a), the training time of good type is less than other quality types because of its less samples. For sparse type in Fig. 11(b), the training time with 100 labeled data is longer

Please cite this article as: F. Huang, et al., Local quality assessment of point clouds for indoor mobile mapping, Neurocomputing (2016), http://dx.doi.org/10.1016/j.neucom.2016.02.033

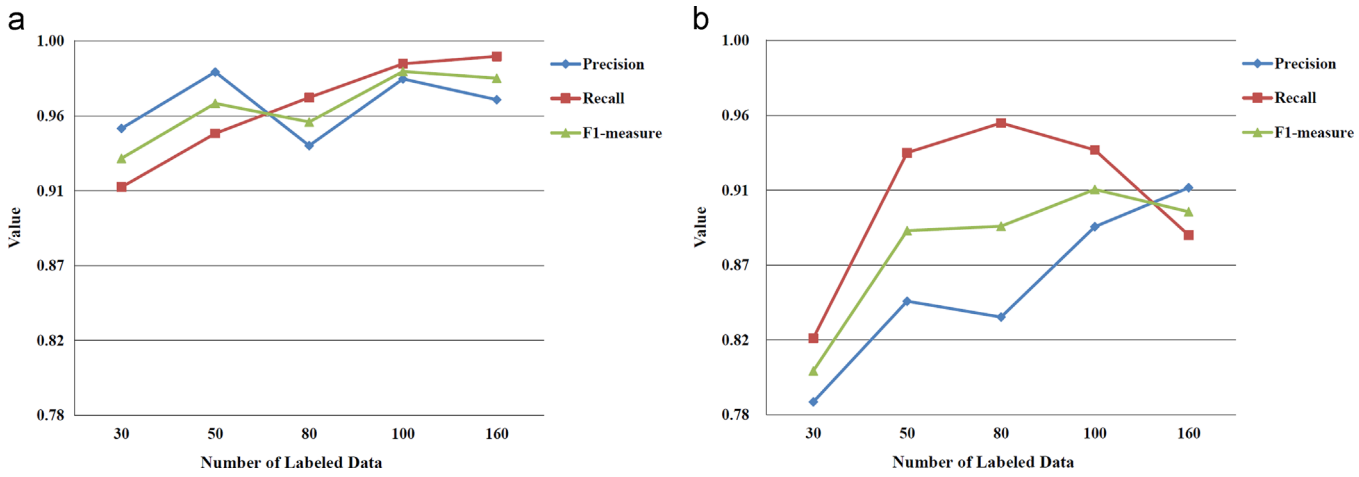

Fig. 9. The precision, recall, and F_1-measure using different numbers of labeled data on the missing type. (a) Our dataset. (b) Cornell dataset.

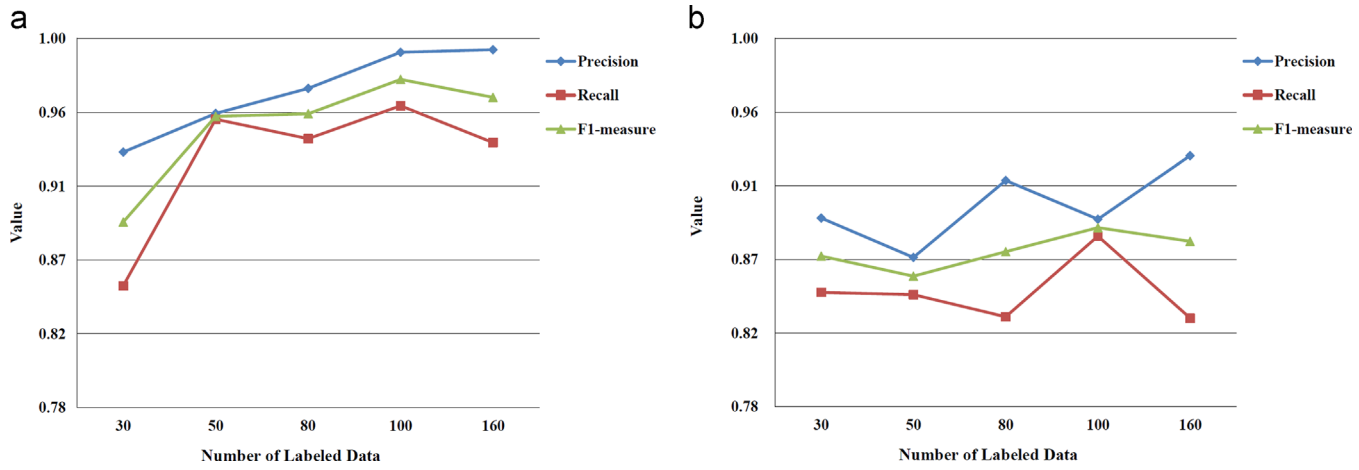

Fig. 10. The precision, recall, and F_1-measure using different numbers of labeled data on the sparse type. (a) Our dataset. (b) Cornell dataset.

than the training time with 80 labeled data. The possible reason is that more iterations required with 100 labeled data than 80 labeled data in the experiment. As a consequence, for Figs. 8–11, the results show that high assessment accuracies are achieved with a small number labeled data (e.g., 30 or 50) using this training model. Furthermore, the more the labeled data are used, the higher the accuracy are achieved and the less training time are required in the experiment. Thus, those figures show that our proposed quality assessment framework can obtain satisfying results in our dataset and the Cornell dataset.

4.4. Performance comparison

In this section, S4VM with supervised and semi-supervised machine learning methods, including Random Forest, Logistic Regression, Bayes Net, KNN, SDA [23], and Hypergraph [24], are compared. To compare the above methods, the same labeled and unlabeled data are used in our experiments. For S4VM, labeled data were first used to learn the labels of unlabeled data; then, updated labels from those unlabeled data were formed in the next iteration. When all of the predicted labels or the optimal separator remain unchanged, or the value of iteration is larger than a default value (e.g., 200 in our experiments), the S4VM training process is terminated. For the Random Forest, Logistic Regression, Bayes Net, and KNN methods, the labeled data are used to train a model. Then, the training model was exploited to predict the labels of unlabeled data. Tables 2 and 3 present the precision, recall and F_1-measure results using 45 feature number selected and 50 labeled data in our dataset and the Cornell dataset, respectively.

As shown in Table 2, the S4VM obtains precision, recall, and F_1-measure with values of 96.6%, 95.0%, and 95.8% on the good type. Furthermore, the S4VM achieves values of 98.1%, 94.5%, and 96.3% on the missing type, and S4VM achieves 95.5%, 95.2%, and 95.3% on the sparse type. SDA achieves a precision value of 98.3%, which is higher than the other methods on the good type. Hypergraph achieves a precision value of 98.4%, which is higher than the other methods on the missing type. On the sparse data type, S4VM obtains the highest precision of 95.5%, which is higher than the other methods. Additionally, the S4VM outperforms all of the other methods on the recall and F_1-measure values. However, S4VM requires longer time to train a model, while the other methods require less time. Hence, S4VM consumes more time to attain the highest performance on our dataset.

Table 3 shows that S4VM obtains the highest recall and F_1-measure values on the good and missing types. Hypergraph has the highest precisions of 87.1% and 86.8% on the good and missing types, respectively. For the sparse type, Bayes Net has the highest precision of 87.9%, while Random Forest has the highest recall of 85.8%, and S4VM has the highest F_1-measure of 85.8%. The results show that S4VM outperforms all other methods on the F_1-measure values. Additionally, S4VM performs slightly better than Random Forest in the sparse type. The possible reason is that the degradation simulation cannot accurately simulate the actual sparse type. Furthermore, S4VM requires a longer time to train a model,

Please cite this article as: F. Huang, et al., Local quality assessment of point clouds for indoor mobile mapping, Neurocomputing (2016), http://dx.doi.org/10.1016/j.neucom.2016.02.033

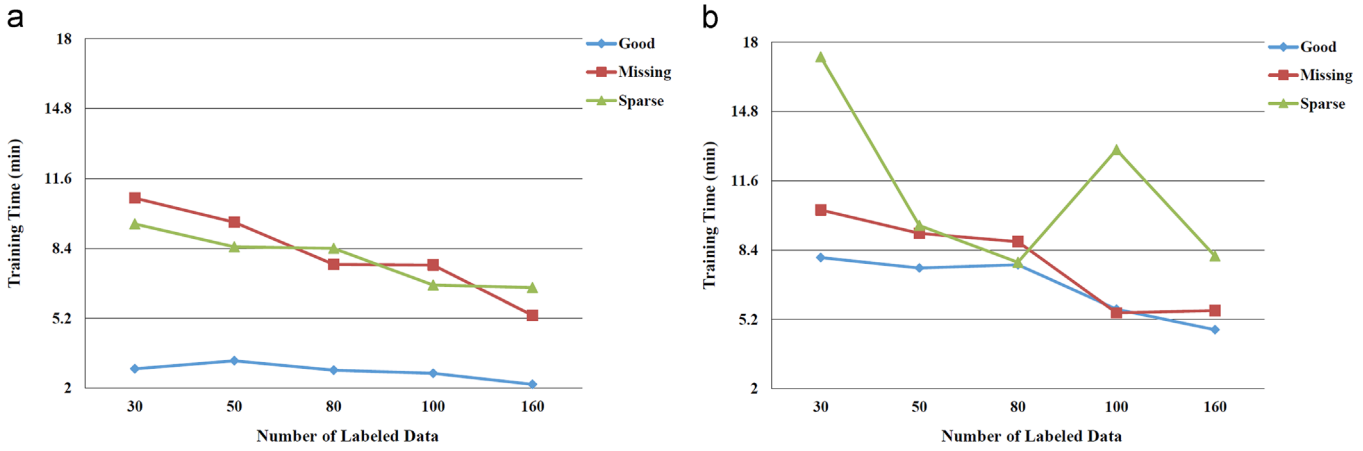

Fig. 11. The relationship between number of labeled data and the corresponding training time on the good, missing, and sparse types. (a) Our dataset. (b) Cornell dataset.

Table 2
Assessment precision, recall, and F_1-measure values using different learning models on our dataset.

Type	Method	Precision (%)	Recall (%)	F_1-measure (%)	Time (s)
Good	Random Forest	86.8	86.5	86.5	0.15
	Logistic	87.7	86.4	86.3	0.28
	Bayes Net	88.8	88.6	88.6	0.14
	KNN	90.6	89.6	89.5	**0.01**
	SDA	**98.3**	90.9	94.4	0.36
	Hypergraph	94.2	92.7	93.4	138.58
	S4VM	96.6	**95.0**	**95.8**	194.81
Missing	Random Forest	88.7	86.8	86.7	0.18
	Logistic	87.3	87.3	87.3	0.31
	Bayes Net	88.4	86.9	86.7	0.15
	KNN	91.3	91.3	91.3	**0.01**
	SDA	95.1	92.4	93.7	0.49
	Hypergraph	**98.4**	92.2	95.2	146.09
	S4VM	98.1	**94.5**	**96.3**	576.57
Sparse	Random Forest	86.1	84.8	84.7	0.16
	Logistic	84.4	83.3	83.1	0.27
	Bayes Net	82.9	82.9	82.9	0.16
	KNN	92.2	91.0	90.9	**0.01**
	SDA	94.9	83.0	88.5	0.51
	Hypergraph	88.6	92.4	90.4	141.57
	S4VM	**95.5**	**95.2**	**95.3**	508.41

Table 3
Assessment precision, recall, and F_1-measure values using different learning models on the Cornell dataset.

Type	Method	Precision (%)	Recall (%)	F_1-measure (%)	Time(s)
Good	Random Forest	83.3	83.2	83.2	0.23
	Logistic	67.4	67.1	67.0	0.07
	Bayes Net	83.3	82.2	82.1	0.04
	KNN	82.9	82.9	82.9	**0.01**
	SDA	81.5	84.9	83.0	0.34
	Hypergraph	**87.1**	70.8	78.1	109.27
	S4VM	85.0	**85.1**	**85.0**	453.54
Missing	Random Forest	81.2	80.2	80.0	0.05
	Logistic	78.6	78.5	78.5	0.07
	Bayes Net	69.8	69.8	69.8	0.04
	KNN	85.6	85	84.9	**0.01**
	SDA	77.4	80.3	78.7	0.29
	Hypergraph	**86.8**	78.2	82.3	87.32
	S4VM	84.7	**93.4**	**88.8**	549.73
Sparse	Random Forest	87	**85.8**	85.7	0.05
	Logistic	77	76.1	75.9	0.07
	Bayes Net	**87.9**	84	83.6	0.03
	KNN	82.7	82	81.9	**0.01**
	SDA	82.9	83.2	82.8	0.49
	Hypergraph	80.9	84.1	82.4	162.78
	S4VM	86.9	84.7	**85.8**	572.16

while the other methods require less time. Hence, we can conclude that S4VM has the highest F_1-measure value but consumes more time on the Cornell dataset.

The above analyses indicate that S4VM is effective and exhibits promising performance for IMMS point cloud quality assessment. However, to build a training model, S4VM requires a longer time than the other methods. The reason is that S4VM has a large iteration time, and each iteration consumes several minutes to update the labels of unlabeled data when generating multiple new representative separators. For example, when the sample size is 100 and each sample process requires 200 iterations, the training process will execute 20,000 iterations in the experiment.

5. Conclusion

In this paper, we proposed a semi-supervised learning framework to solve the problem of local quality assessment of IMMS point clouds with limited labeled data and a large amount of unlabeled data. First, we collected IMMS point cloud data by a depth camera mounted on a mobile robot, and created a point cloud dataset with multiple kinds of quality problems. Next, we used feature extraction and feature selection methods to obtain optimal feature sets that are exploited to describe local degradation. Finally, we introduced a semi-supervised machine learning method to predict the labels of unlabeled data by learning from limited labeled data and a large amount of unlabeled data. Our experimental results demonstrated significant effectiveness and efficiency in the proposed quality assessment framework for indoor mobile mapping point clouds. Future work will be focused on repairing low quality point clouds based on the point cloud quality assessment results, in which different repair strategies will be utilized based on the different degraded types.

Acknowledgments

This work is supported by the National Science Foundation of China (Grant no. 61401382).

Please cite this article as: F. Huang, et al., Local quality assessment of point clouds for indoor mobile mapping, Neurocomputing (2016), http://dx.doi.org/10.1016/j.neucom.2016.02.033

References

[1] S. Izadi, D. Kim, O. Hilliges, D. Molyneaux, R. Newcombe, P. Kohli, J. Shotton, S. Hodges, D. Freeman, A. Davison, KinectFusion: real-time 3D reconstruction and interaction using a moving depth camera, in: Proceedings of the 24th Annual ACM Symposium on User Interface Software and Technology, ACM, 2011, pp. 559–568.
[2] Y. Tian, Y. Long, D. Xia, H. Yao, J. Zhang, Handling occlusions in augmented reality based on 3D reconstruction method, Neurocomputing 156 (2015) 96–104.
[3] C. Wang, J. Yu, D. Tao, High-level attributes modeling for indoor scenes classification, Neurocomputing 121 (2013) 337–343.
[4] R.B. Rusu, N. Blodow, Z.C. Marton, M. Beetz, Close-range scene segmentation and reconstruction of 3D point cloud maps for mobile manipulation In domestic environments, in: Proceedings of the IEEE/RSJ International Conference on Intelligent Robots and Systems, 2009. IROS 2009, IEEE, 2009, pp. 1–6.
[5] M. Ye, Y. Zhang, R. Yang, D. Manocha, 3D reconstruction in the presence of glasses by acoustic and stereo fusion, In: Proceedings of the IEEE Conference on Computer Vision and Pattern Recognition, 2015, pp. 4885–4893.
[6] N. Corso, A. Zakhor, Indoor localization algorithms for an ambulatory human operated 3D mobile mapping system, Remote Sens. 5 (2013) 6611–6646.
[7] C. Wen, L. Qin, Q. Zhu, C. Wang, J. Jonathan Li, Three-dimensional indoor mobile mapping with fusion of two-dimensional laser scanner and RGB-D camera data, IEEE Geosci. Remote Sens. Lett. 11 (2014) 843–847.
[8] M. Bosse, R. Zlot, P. Flick, Zebedee: Design of a spring-mounted 3-d range sensor with application to mobile mapping, IEEE Trans. Robot. 28 (2012) 1104–1119.
[9] P. Henry, M. Krainin, E. Herbst, X. Ren, D. Fox, RGB-D mapping: using Kinect-style depth cameras for dense 3D modeling of indoor environments, Int. J. Robot. Res. 31 (2012) 647–663.
[10] T. Liu M. Carlberg G. Chen J. Chen J. Kua A. Zakhor Indoor localization and visualization using a human-operated backpack system In: Proceedings of the 2010 International Conference onIndoor Positioning and Indoor Navigation (IPIN), IEEE, 2010, pp. 1–10.
[11] Y.-F. Li, Z.-H. Zhou, Towards making unlabeled data never hurt, IEEE Trans. Pattern Anal. Mach. Intell. 37 (2015) 175–188.
[12] W. Xue, L. Zhang, X. Mou, Learning without human scores for blind image quality assessment, In: Proceedings of the 2013 IEEE Conference on Computer Vision and Pattern Recognition (CVPR), IEEE, 2013, pp. 995–1002.
[13] C. Zhang, J. Pan, S. Chen, T. Wang, D. Sun, No reference image quality assessment using sparse feature representation in two dimensions spatial correlation, Neurocomputing 173 (2016) 462–470.
[14] Y. Yuan, Q. Guo, X. Lu, Image quality assessment: a sparse learning way, Neurocomputing 159 (2015) 227–241.
[15] H. Tang, N. Joshi, A. Kapoor, Blind image quality assessment using semi-supervised rectifier networks, In: Proceedings of the 2014 IEEE Conference on Computer Vision and Pattern Recognition (CVPR), IEEE, 2014, pp. 2877–2884.
[16] Y. Li, L.-M. Po, X. Xu, L. Feng, F. Yuan, C.-H. Cheung, K.-W. Cheung, No-reference image quality assessment with shearlet transform and deep neural networks, Neurocomputing 154 (2015) 94–109.
[17] S.O. Elberink, G. Vosselman, Quality analysis on 3D building models reconstructed from airborne laser scanning data, ISPRS J. Photogramm. Remote Sens. 66 (2011) 157–165.
[18] E.B. Anil, P. Tang, B. Akinci, D. Huber, Deviation analysis method for the assessment of the quality of the as-is building information models generated from point cloud data, Autom. Constr. 35 (2013) 507–516.
[19] J. Feng, R. Zhong, Y. Yang, W. Zhao, Quality evaluation of spatial point-cloud data collected by vehicle-borne laser scanner, In: Proceedings of the International Workshop on Education Technology and Training, 2008. and 2008 International Workshop on Geoscience and Remote Sensing. ETT and GRS 2008, IEEE, 2008, pp. 320–323.
[20] A. Habib, A.P. Kersting, K.I. Bang, D. Lee, Alternative methodologies for the internal quality control of parallel LiDAR strips, IEEE Trans. Geosci. Remote Sens. 48 (2010) 221–236.
[21] K. Khoshelham, S.O. Elberink, Accuracy and resolution of kinect depth data for indoor mapping applications, Sensors 12 (2012) 1437–1454.
[22] K. Khoshelham, Accuracy analysis of kinect depth data, In: Proceedings of the ISPRS workshop laser scanning, 2011, p. W12.
[23] D. Cai, X. He, J. Han, Semi-supervised discriminant analysis In: Proceedings of the IEEE 11th International Conference on Computer Vision, 2007. ICCV 2007, IEEE, 2007, pp. 1–7.
[24] J. Yu, D. Tao, M. Wang, Adaptive hypergraph learning and its application in image classification, IEEE Trans. Image Process. 21 (2012) 3262–3272.
[25] J. Yu, Y. Rui, Y.Y. Tang, D. Tao, High-order distance-based multiview stochastic learning in image classification, IEEE Trans. Cybern. 44 (2014) 2431–2442.
[26] J. Yu, D. Tao, M. Wang, Y. Rui, Learning to rank using user clicks and visual features for image retrieval, IEEE Trans. Cybern. 45 (2015) 767–779.
[27] J. Yu, Y. Rui, D. Tao, Click prediction for web image reranking using multimodal sparse coding, IEEE Trans. Image Process. 23 (2014) 2019–2032.
[28] X. Liu, M. Wang, B.-C. Yin, B. Huet, X. Li, Event-Based Media Enrichment Using an Adaptive Probabilistic Hypergraph Model, IEEE Trans. Cybern. 45 (2015) 2461–2471.
[29] M. Wang, X.-S. Hua, R. Hong, J. Tang, G.-J. Qi, Y. Song, Unified video annotation via multigraph learning, IEEE Trans. Circuits Syst. Video Technol. 19 (2009) 733–746.
[30] M. Wang, X. Wu, Visual Classification by l1-Hypergraph Modeling, IEEE Trans. Knowl. Data Eng. 27 (2015) 2564–2574.
[31] B. Wei, M. Cheng, C. Wang, J. Li, Combinative hypergraph learning for semi-supervised image classification, Neurocomputing 153 (2015) 271–277.
[32] B. Steder, R.B. Rusu, K. Konolige, W. Burgard, NARF: 3D range image features for object recognition, in: Proceedings of the Workshop on Defining and Solving Realistic Perception Problems in Personal Robotics at the IEEE/RSJ International Conference on Intelligent Robots and Systems (IROS), 2010.
[33] R.B. Rusu, N. Blodow, M. Beetz, Fast point feature histograms (FPFH) for 3D registration, In: Proceedings of the IEEE International Conference on Robotics and Automation, 2009. ICRA'09, IEEE, 2009, pp. 3212–3217.
[34] A.E. Johnson, M. Hebert, Using spin images for efficient object recognition in cluttered 3D scenes, IEEE Trans. Pattern Anal. Mach. Intell. 21 (1999) 433–449.
[35] D. Munoz, N. Vandapel, M. Hebert, Onboard contextual classification of 3-d point clouds with learned high-order markov random fields, In: Proceedings of the IEEE International Conference on Robotics and Automation. ICRA'09, IEEE, 2009.
[36] R. Schnabel, R. Wahl, R. Klein, Efficient RANSAC for point-cloud shape detection in: Proceedings of the Computer Graphics Forum, Wiley Online Library, 2007, pp. 214–226.
[37] A. Anand, H.S. Koppula, T. Joachims, A. Saxena, Contextually guided semantic labeling and search for three-dimensional point clouds, Int. J. Robot. Res. (2012) 0278364912461538.
[38] H.S. Koppula, A. Anand, T. Joachims, A. Saxena, Semantic labeling of 3d point clouds for indoor scenes In: Proceedings of the Advances in Neural Information Processing Systems, 2011, pp. 244–252.
[39] ⟨http://pr.cs.cornell.edu/sceneunderstanding/data/data.php⟩.
[40] K.J. Archer, R.V. Kimes, Empirical characterization of random forest variable importance measures, Comput. Stat. Data Anal 52 (2008) 2249–2260.
[41] A. Verikas, A. Gelzinis, M. Bacauskiene, Mining data with random forests: A survey and results of new tests, Pattern Recognit. 44 (2011) 330–349.
[42] M.B. Kursa, W.R. Rudnicki, Feature Selection with the Boruta Package, In: Journal, 2010.
[43] M.B. De Almeida, A. de Pádua Braga, J.P. Braga, SVM-KM: speeding SVMs learning with a priori cluster selection and k-means, In: Proceedings of the Sixth Brazilian Symposium on Neural Networks, 2000, pp. 162–167.
[44] ⟨http://docs.pointclouds.org/trunk/classpcl_1_1_voxel_grid.html⟩.

Fangfang Huang received the B.Sc degree in computer science from Fuzhou University, China in 2013. She is currently a master student with the Fujian Key Laboratory of Sensing and Computing for Smart City in the School of Information Science and Engineering, Xiamen University, China. Her current research interests include computer vision, machine learning, and mobile LiDAR point clouds data processing.

Chenglu Wen received the Ph.D. degree in mechanical engineering from China Agricultural University, Beijing, China in 2009. She is currently an Associate Professor with Fujian Key Laboratory of Sensing and Computing for Smart City, School of Information Science and Engineering, Xiamen University, Xiamen, China. She has coauthored more than 30 research papers published in refereed journals and proceedings. Her current research interests include machine vision, machine learning, and point cloud processing. She is the secretary of ISPRS WG I/3 on Multi-Platform Multi-Sensor System Calibration (2012–2016).

Huan Luo received the B.Sc degree in software engineering from Nanchang University, China in 2009. He is currently a Ph.D. student with the Fujian Key Laboratory of Sensing and Computing for Smart City in the School of Information Science and Engineering, Xiamen University, China. His current research interests include computer vision, machine learning, and mobile LiDAR point clouds data processing.

Please cite this article as: F. Huang, et al., Local quality assessment of point clouds for indoor mobile mapping, Neurocomputing (2016), http://dx.doi.org/10.1016/j.neucom.2016.02.033

Ming Cheng received the Ph.D. degree in Biomedical Engineering from Tsinghua University, China in 2004. He is currently an Associate Professor with the Fujian Key Laboratory of Sensing and Computing for Smart Cities, School of Information Science and Engineering, Xiamen University, China. His research interests include remote sensing image processing, computer vision, and machine learning.

Cheng Wang received the Ph.D. degree in information and communication engineering from the National University of Defense Technology, Changsha, China in 2002. He is currently a Professor with and the Associate Dean of the School of Information Science and Technology, Xiamen University, Xiamen, China. He has authored more than 80 publications. His research interests include remote sensing image processing, mobile LiDAR data analysis, and multisensor fusion. He is a council member of China Society of Image and Graphics, IEEE Senior Member, and Co-Chair of ISPRS Working Group I/3 on Multi-Platform Multi-Sensor System Calibration (2012-2016).

Jonathan Li received the Ph.D. degree in geomatics engineering from the University of Cape Town, Cape Town, South Africa. He is currently a Professor with the Fujian Key Laboratory of Sensing and Computing for Smart Cities, School of Information Science and Engineering, Xiamen University, China. He is also Professor and Head of the Mobile Sensing and Geodata Science Lab at the University of Waterloo, Canada. He has co-authored more than 300 publications, over 130 of which were published in refereed journals, including IEEE-TGRS, IEEE-JSTARS, IEEE-TITS, IEEE-GRSL, ISPRS-JPRS, IJRS, PE&RS, and RSE. His current research interests include information extraction from mobile LiDAR point clouds and from Earth observation images. Prof. Li is the Chair of the ISPRS Working Group I/Va on Mobile Scanning and Imaging Systems (2012-2016), Chair of the ICA Commission on Sensor-driven Mapping (2015-2019), and Associate Editor of IEEE-TITS, IEEE-JSARRS and Geomatica.

Please cite this article as: F. Huang, et al., Local quality assessment of point clouds for indoor mobile mapping, Neurocomputing (2016), http://dx.doi.org/10.1016/j.neucom.2016.02.033